Since January 2020 Elsevier has created a COVID-19 resource centre with free information in English and Mandarin on the novel coronavirus COVID-19. The COVID-19 resource centre is hosted on Elsevier Connect, the company's public news and information website.

Free Radical Biology and Medicine 161 (2020) 15–22

Contents lists available at ScienceDirect

Free Radical Biology and Medicine

journal homepage: www.elsevier.com/locate/freeradbiomed

Original article

Control of systemic inflammation through early nitric oxide supplementation with nitric oxide releasing nanoparticles

Alexander T. Williams[a], Cynthia R. Muller[a], Krianthan Govender[a], Mahantesh S. Navati[b], Adam J. Friedman[c], Joel M. Friedman[b], Pedro Cabrales[a,*]

[a] Department of Bioengineering, University of California San Diego, La Jolla, CA, 92093, USA
[b] Department of Physiology and Biophysics, Albert Einstein College of Medicine, Bronx, NY, 10461, USA
[c] Department of Dermatology, George Washington University School of Medicine, Washington DC, USA

ARTICLE INFO

Keywords:
Inflammation
Sepsis
Septic shock
Vascular permeability
Nitric oxide
Cytokine storm

ABSTRACT

Amelioration of immune overactivity during sepsis is key to restoring hemodynamics, microvascular blood flow, and tissue oxygenation, and in preventing multi-organ dysfunction syndrome. The systemic inflammatory response syndrome that results from sepsis ultimately leads to degradation of the endothelial glycocalyx and subsequently increased vascular leakage. Current fluid resuscitation techniques only transiently improve outcomes in sepsis, and can cause edema. Nitric oxide (NO) treatment for sepsis has shown promise in the past, but implementation is difficult due to the challenges associated with delivery and the transient nature of NO. To address this, we tested the anti-inflammatory efficacy of sustained delivery of exogenous NO using i.v. infused NO releasing nanoparticles (NO-np). The impact of NO-np on microhemodynamics and immune response in a lipopolysaccharide (LPS) induced endotoxemia mouse model was evaluated. NO-np treatment significantly attenuated the pro-inflammatory response by promoting M2 macrophage repolarization, which reduced the presence of pro-inflammatory cytokines in the serum and slowed vascular extravasation. Combined, this resulted in significantly improved microvascular blood flow and 72-h survival of animals treated with NO-np. The results from this study suggest that sustained supplementation of endogenous NO ameliorates and may prevent the morbidities of acute systemic inflammatory conditions. Given that endothelial dysfunction is a common denominator in many acute inflammatory conditions, it is likely that NO enhancement strategies may be useful for the treatment of sepsis and other acute inflammatory insults that trigger severe systemic pro-inflammatory responses and often result in a cytokine storm, as seen in COVID-19.

1. Introduction

Sepsis represents a dynamic progression of host-pathogen interactions that progressively causes a systemic inflammatory response syndrome (SIRS) and ultimately leads to multi-organ dysfunction syndrome (MODS) even after the initial insult has been controlled [1]. The complications associated with sepsis are the most common cause of death in non-coronary intensive care units (ICUs) worldwide. Medical care costs related to sepsis treatment add up to approximately $20 billion in the United States [2,3]. However, the development of a comprehensive study to target key aspects of sepsis development and progression has been challenging and most of the results obtained from bench top experiments are hard to translate to the bedside. The difficulty to generate translatable data in experimental studies comes mainly from two reasons. First, the large number of variables that play a role in the deterioration of cell and tissue function during SIRS and sepsis makes it almost impossible to pinpoint a single therapeutic target [3,4]. Second, the complexity and diverse sources of human sepsis makes the development of an animal model that is reproducibly translatable, in which different theories could be tested, almost impossible. Thus, a middle ground should be set in which individual components of sepsis can be used to understand the response of the insulted organism.

A well-described hallmark of sepsis is endothelial dysfunction in response to a cytokine 'storm', which is associated with an increase in a series of negative consequences arising from overproduction of reactive oxygen species (ROS), disruption of the glycocalyx, and endothelial nitric oxide synthase (eNOS) uncoupling, all contributing to increased adhesion of red blood cells (RBCs), white blood cells (WBCs), and platelets to the endothelium lining, enhanced platelet activation, blood

* Corresponding author. University of California San Diego, Department of Bioengineering, 9500 Gilman Dr, La Jolla, CA, 92093-0412, USA.
E-mail address: pcabrales@ucsd.edu (P. Cabrales).

https://doi.org/10.1016/j.freeradbiomed.2020.09.025
Received 6 July 2020; Received in revised form 18 September 2020; Accepted 28 September 2020
Available online 02 October 2020
0891-5849/

stagnation, decreased tissue perfusion and increased vascular permeability [1,5,6]. Experimental therapies designed to target this aspect have been promising and represent pathways that could be targeted to increase survival [5,6]. From a clinical standpoint, several studies have highlighted that microvascular function is drastically impaired in patients in different stages of sepsis [7]. The evidence indicates that the gold standard, fluid replacement therapies, fail to recover microvascular blood flow causing poor perfusion, which has been associated with increased mortality [8,9]. Routinely monitored clinical variables poorly reflect the true state of the microcirculation in central and peripheral tissues [10]. Recently it has been proposed that in order to properly restore cardiovascular homeostasis, the microcirculation should be targeted as a functional unit [11–13]. Thus, the understanding of different components of SIRS and sepsis should be assessed from a microvascular perspective in addition to traditional bench top tissue culture studies.

In this work, we present a murine window chamber model for the study of the microvascular hemodynamics and endothelial barrier integrity upon intravascular administration of lipopolysaccharides (LPS). The window chamber model allows for the direct quantification of microhemodynamics and transport phenomena in an intact tissue of an unanesthetized animal. LPS is a component of the membrane of gram-negative bacteria, and it is recognized by all cell types via toll-like receptor 4 (TLR4), a major component of innate immunity [14]. Upon TLR4 activation a complex inflammatory cascade is activated and thus, LPS injection has been largely used as an experimental model of sepsis [15]. However, because it does not closely replicate most of the features of human sepsis, it has also been largely criticized [15]. In this study however, we propose single bolus i.v. injection of LPS as a valid and robust way to understand the early responses of microvascular hemodynamics and endothelial barrier integrity upon exposure to an inflammatory agent. We hypothesized that LPS-induced endotoxemia would result in a derangement in microvascular blood flow, tissue perfusion, and endothelial glycocalyx integrity and that NO supplementation would reverse these changes. To examine this hypothesis, we combined the window chamber model with state-of-the-art engineering methods to quantify phenomena occurring in the microvascular bed shortly after LPS infusion with and without exogenous NO supplementation.

2. Methods

2.1. Nanoparticle preparation and characterization

The tetramethoxysilane derived hydrogel based NO releasing nanoparticles used in this study were prepared as described in several previous publications as was the characterization [16]. Based on the results from earlier optimization studies in a variety of rodent models, the dosing chosen was 10 mg/kg of animal weight [17,18].

2.2. Animal preparation

Male, Balb/c mice (23–28 g, Jackson Laboratory) were used for this experimental study. All the procedures including animal handling and care followed the National Institute of Health (NIH) Guide for the Care and Use of Laboratory Animals. The UC San Diego Institutional Animal Care and Use Committee approved the experimental protocol. The mice were fitted with a dorsal skinfold window chamber for direct visualization of an intact microvascular bed. This model has been widely used to characterize the perfusion of peripheral tissues in different clinically relevant scenarios in unanesthetized animals as described elsewhere [19,20]. Briefly, the animals are anesthetized with an i.p. injection of 50 mg/kg pentobarbital sodium, the dorsal area is depilated, and a skinfold is lifted away from the back using sutures. The window chamber consists of two titanium frames with a circular opening for visualization, each one of which is secured to each side of the skinfold. The skin on one of the sides is removed following the outline of the circular window. Finally, the exposed skin is covered with a glass coverslip under a drop of saline. After the window chamber was implanted the animals were left for at least 2 days to recover, after which they underwent surgery again for arterial (carotid) catheter implantation (PE50 tubing). The animals were allowed 2 more days for recovery before any experimental procedure was performed.

2.3. Inclusion criteria

Animals were considered suitable for the experiments if: 1) systemic parameters were within normal range, namely, heart rate (HR) $>$ 350 beats/min, mean arterial blood pressure (MAP) $>$ 80 mmHg and, 2) microscopic examination of the tissue in the window chamber observed under 650^{x} magnification did not reveal signs of edema or bleeding.

2.4. Experimental protocol

All animals were prepared following the same surgical interventions, housed under the same conditions (12-h day/night cycle, approximately 24 °C and 60% humidity) until the day of experimentation, and only animals that fulfilled the inclusion criteria were used in this study. Baseline parameter were collected after 15 min of adaptation to the experimental conditions. Animals received 10 mg/kg of lipopolysaccharide (LPS) from e. coli serotype 0128:B12 (Sigma Aldrich St. Louis, MO) suspended in 100 μL of saline solution (0.9% NaCl) via arterial catheter. LPS solution was prepared fresh every day before the experiments. Treatments were administered 30 min after LPS infusion, no additional fluid therapies were applied. Food and water were available between observation time points (1 h, 2 h, 6 h and 24 h). Animals were followed over 72 h to assess survival.

2.5. Experimental groups

Animals were divided into two experimental groups, named based on the treatments, NO-np (10 mg/kg, NO releasing nanoparticles), and Control-np (10 mg/kg, nanoparticles without NO). All doses were calculated based on tetramethoxysilane concentration of each formulation. Treatments were infused intra-arterial and all groups received equal volume of saline solution to suspend the nanoparticles (100 μL).

2.6. Systemic parameters

MAP and HR were monitored throughout the experiment using the arterial line and a transducer-computer interface (MP 150; Biopac System, Santa Barbara, CA).

2.7. Intravital microscopy and microvascular measurements

The window chamber was studied using transillumination on a custom intravital microscope. Briefly, the animals were restrained in a plexiglass tube with a longitudinal opening from which the window protruded and then they were fixed to the stage of an upright microscope (BX51WI, Olympus, New Hyde Park, NY) as described and depicted elsewhere [20]. Measurements were carried out using a 40^{x} (LUMPFL-WIR, numerical aperture 0.8, Olympus) water immersion objective. The microscope was equipped with a high-speed video camera (Fastcam 1024 PCI, Photron USA), which was used to record videos of the microvascular blood flow at 1000 frames per second (fps). Briefly, at the beginning of the experiment a macro picture of the window chamber is taken and used to identify arterioles and venules, usually 3 to 4 arterioles and 4 to 5 venules are chosen on each chamber. The same vessels are followed throughout the entire experiment to allow comparisons at different time points. The selected vessels are focused and a video of the flow on each vessel is recorded and stored on a hard drive for offline analysis as described previously by our group to

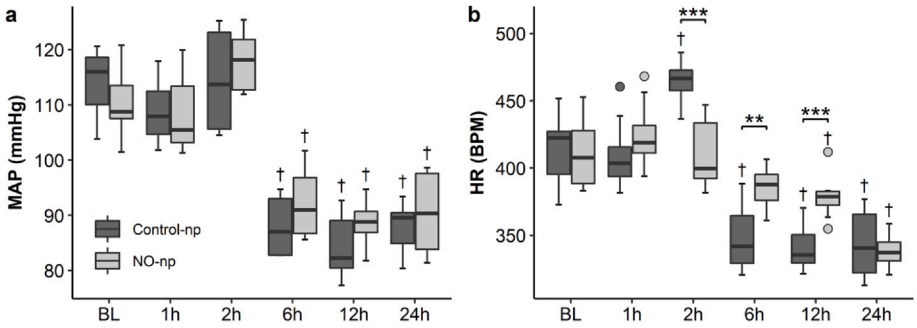

Fig. 1. Central hemodynamics of mice before (BL) and after dosage with LPS and nanoparticles. (a) Mean arterial pressure significantly decreased 6 h after LPS dosage. (b) NO-np treatment normalized changes in HR following LPS dosage. N = 8/group. *p < 0.05, **p < 0.01, ***p < 0.001, and ****p < 0.0001 between groups; †p < 0.05 vs BL.

determine vascular diameter and flow [21].

2.8. Capillary perfusion

Functional capillary density (FCD) was measured by counting the number of capillaries with RBC transit of at least one cell in a 45s period. Ten consecutive microscope visualization fields are selected at baseline and monitored at the different time points throughout the experiment. FCD is defined as the total length of red blood cell (RBC) perfused capillaries divided by the area of the microscopic fields (cm^{-2}).

2.9. Endothelial barrier permeability

The microvascular wall permeability was assessed by measuring the rate of extravasation of fluorescein isothiocyanate-conjugated dextran (FITC-Dextran-70 kDa MW; Sigma, St. Louis, MO). The animals received a single 100 μL bolus of FITC-Dextran diluted in saline solution (10 mg/mL) via the tail vein, which was used to measure extravasation for the entire experimental period. The dye circulated for 5 min and locations of interest showing arterioles, venules and tissue space were selected prior to fluorescent imaging sessions. The tissue was excited using a standard FITC filter cube and images were recorded using the same microscope and animal restraint described above, but equipped with a high light-sensitivity camera (C4742-95, Hamamatsu photonics). Images of the regions of interest were recorded 30 min, 2 h, and 24 h post-LPS injection, keeping the camera exposure time constant throughout the experiment. The images were analyzed offline by measuring the relative pixel intensity inside the microvessels and in the tissue adjacent to the vessel walls. The data is presented as the ratio between the extravascular (I_0) intensity and the intravascular intensity (I_i), high ratios indicate increased vascular permeability.

2.10. Macrophage collection and flow cytometry

After mice were sacrificed, their peritoneal macrophages were isolated by lavage with 4 mL of ice-cold PBS with 10 IU/mL heparin and 10% fetal bovine serum (Sigma Aldrich). The abdomen was gently massaged, and the fluid was aspirated. After centrifugation at 1200 rpm for 5 min at 4 °C, cells were rinsed with cold DMEM. The pellet was then resuspended in fluorescence-activated cell sorting (FACS) buffer containing HBSS with 0.3 μM EDTA and 0.2% FBS, and stained for 30 min with biotinylated anti-MerTK, followed by conjugated antibodies (CD14, clone Sa2-8, conjugated to PerCP-Cy5.5, CD163, clone GHI/61, conjugated to eF450; CD11c, clone N418 conjugated to PE-Cy7; CD206, clone 19.2 (RUO), conjugated to FITC) for another 30 min. FACS data were acquired using the FACS Aria flow cytometer (BD Biosciences), and data were analyzed with FlowJo software (Ashland, Oregon).

2.11. Cytokine measurements

Plasma samples collected from different animals at multiple timepoints were analyzed using an Inflammatory Cytokine enzyme-linked immunosorbent assay (ELISA) Kit (Multiplex mice cytokine ELISA Kit, R&D Systems) according to the manufacturer's instructions.

2.12. Statistical analysis

Results are presented as Tukey boxplots or as mean ± deviation. Data within each group and between time points were analyzed using two-way analysis of variance (ANOVA). When appropriate, post hoc analyses were performed with Tukey's multiple comparison test. All statistics were calculated using R version 3.6.3 (R Core Team, Vienna, Austria). Changes were considered statistically significant if $p < 0.05$.

3. Results

3.1. Systemic hemodynamics

Changes in systemic hemodynamics are presented in Fig. 1. Both animals treated with Control-np and NO-np had similar changes in mean arterial pressure (MAP) in response to LPS dosage. There were no changes in MAP for the initial 2 h following LPS dosage, but after 6 h, there was a profound (nearly 25%) and prolonged decrease in MAP that lasted until the 24-h end point. There was no change in heart rate (HR) for either group for the first hour, but after 2 h, animals treated with Control-np had significantly higher HR than at baseline. By 6 h, animals treated with Control-np had a significant and sustained decrease in HR until the end of the experimental protocol. Treatment with NO-np ameliorated the changes in HR that were induced by LPS dosage, and maintained significantly higher HR than animals dosed with Control-np, until the 24-h end point. There was a downward trend of HR for NO-np-treated animals over time, but there were no statistically significant differences until the 12-h time point.

3.2. Microhemodynamics

To characterize microvascular response to LPS dosage and nanoparticle treatment, we characterized changes in arteriolar diameter and flow, and these changes are presented in Fig. 2. Arteriolar diameter had a faster response to LPS dosage than systemic hemodynamics. Both groups experienced significant microvascular vasodilation at the 2-h time point, while systemic hemodynamic changes were not apparent until the 6-h time point. There were no significant differences in arteriolar diameter between groups at any time point. After 2 h, animals treated with Control-np experienced a significant decrease in arteriolar flow compared to baseline, but animals treated with NO-np maintained baseline levels of arteriolar flow until 6 h post LPS dosage. 12 h and 24 h after LPS dosage, all animals had significantly decreased flow compared to baseline, but NO-np treated animals had significantly higher flow than their control counterparts at these time points.

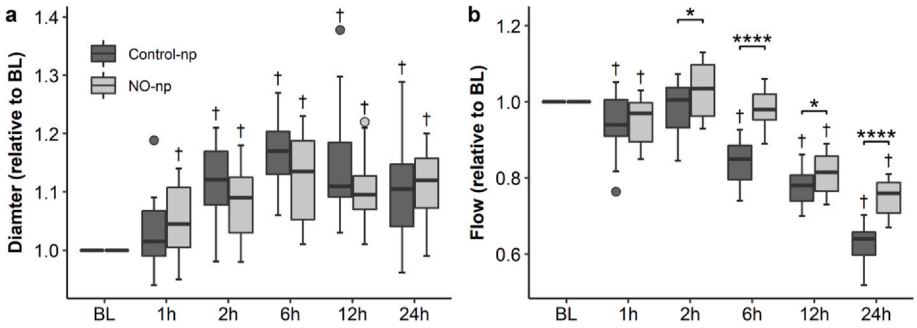

Fig. 2. Arteriolar microhemodynamics of mice after dosage with LPS, relative to baseline. Microhemodynamic aberrations appear more rapidly than changes in systemic hemodynamics. (a) LPS dosage results in vasodilation systemically, independent of treatment. (b) Flow decreases following LPS treatment, but NO-np treatment partially prevents this decrease in flow. N = 22 vessels/group. *p < 0.05, **p < 0.01, ***p < 0.001, and ****p < 0.0001 between groups; †p < 0.05 vs BL.

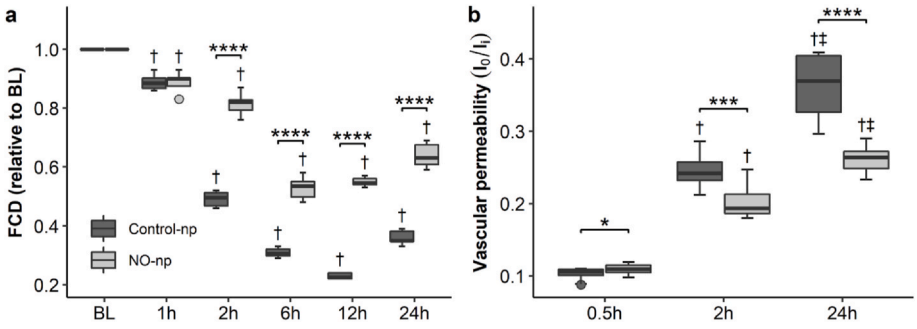

Fig. 3. Changes in functional capillary density (FCD) and vascular permeability after LPS dosage. (a) Treatment with NO-np increased FCD significantly compared to Control-np, thus improving capillary flow and microvascular O_2 transport; N = 8/group. (b) NO-np attenuated the increased permeability compared to animals that received Control-np. I_0 and I_i are the extravascular and intravascular intensity of FITC, respectively. (c) Representative image of the changes in vascular permeability. N = 12/group. *p < 0.05, **p < 0.01, ***p < 0.001, and ****p < 0.0001 between groups; †p < 0.05 vs BL or 0.5 h; ‡p < 0.05 vs 2 h.

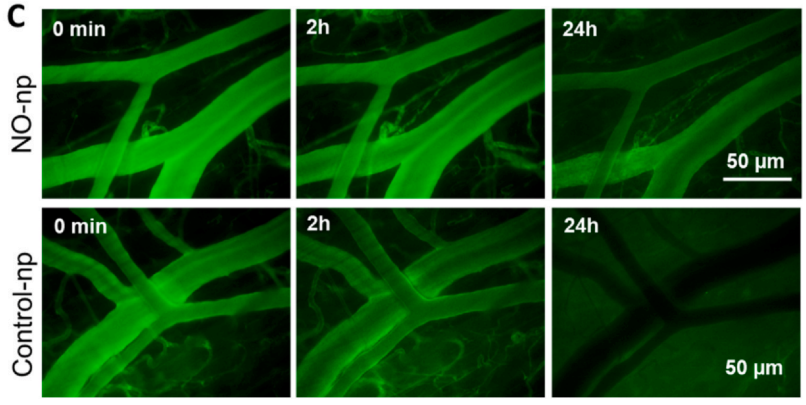

3.3. Functional capillary density

Changes in FCD are presented in Fig. 3a. FCD decreased significantly in response to LPS treatment after only 1 h. FCD decreased more than 50% for animals treated with Control-np 2 h after LPS dosage, and this decrease in FCD continued for the length of the observation period. Animals dosed with NO-np also experienced a significant decrease in FCD compared to baseline, but NO-np treatment maintained significantly higher FCD compared to animals treated with Control-np.

3.4. Vascular permeability

LPS dosage caused a significant increase in vascular permeability, as indicated by the rate of FITC extravasation, shown in Fig. 3b and c. 30 min post-LPS dosage, animals treated with NO-np showed a small (but significant) increase in extravascular fluorescent intensity ratio compared to control animals. After 2 h, extravascular fluorescent intensity ratio increased 2.4 × for Control-np but only 1.9 × for NO-np compared to the 30-min time point, and the extravascular fluorescent intensity ratio was significantly lower for NO-np than Control-np. After 24 h, extravascular fluorescent intensity ratio for Control-np was 3.5 × higher than the 30-min time point, whereas extravascular fluorescent intensity ratio was 2.4 × higher than the 30-min time point for NO-np. At 24 h, extravascular fluorescent intensity ratio for NO-np's was comparable to that of Control-np's at 2 h.

3.5. Survival

In addition to measuring functional parameters, we also assessed survival of mice dosed with LPS over 72 h (Fig. 4). NO-np treatment significantly improved survival compared to mice treated with Control-np. Mice treated with Control-np started dying after 40 h, whereas the first (and only) death of NO-np treated mice occurred 68 h after LPS dosage. Additionally, less than 20% of animals pretreated with Control-np survived the full 72 h, while all but one NO-np treated mouse survived for 72 h.

3.6. Peritoneal macrophage phenotype

Peritoneal macrophages were subjected to FACS to determine the phenotype of macrophages circulating 72 h after LPS dosage and nanoparticle treatment, shown in Fig. 5. FACS revealed that macrophages of animals treated with Control-np contained high counts of the surface marker CD11c, and low counts of CD206, indicating an M1-like macrophage phenotype, which is considered to be inflammatory. In fact,

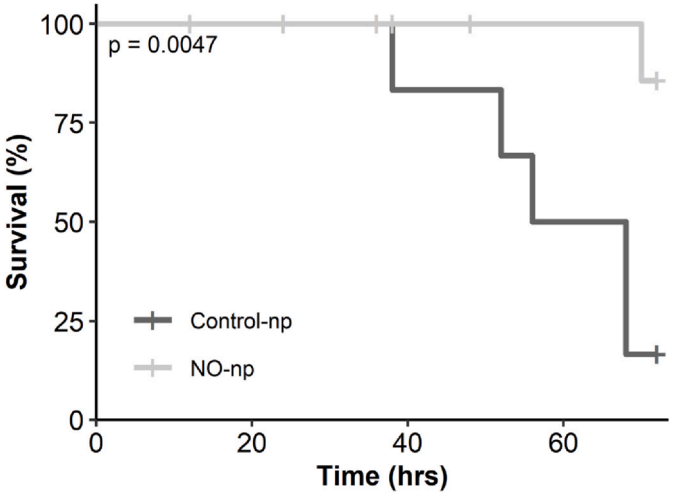

Fig. 4. Survival curve over 72 h of animals treated with Control and NO-nps after LPS dosage. NO-np significantly improved 72-h survival, with only one animal dying over the observation period. Significance was measured via Log-Rank test. N = 9 & 12 at time = 0 for Control-np and NO-np, respectively.

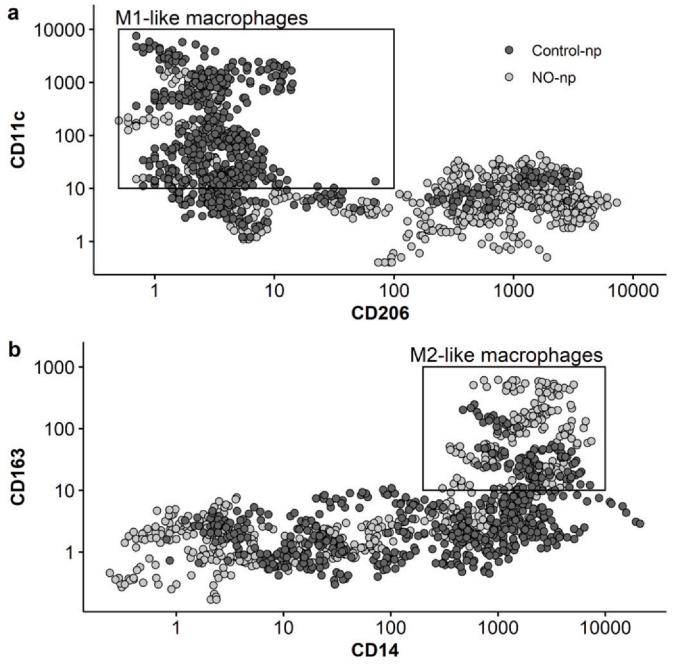

Fig. 5. Fluorescence-activated cell sorting (FACS) of peritoneal macrophages from LPS-dosed animals after 72 h reveals that macrophages from Control-np had a primarily M1-like (inflammatory) phenotype, with M1-like macrophages representing 72% of all macrophages for Control-np, but only 16% of all macrophages for NO-np (a), but significantly more macrophages from animals treated with NO-np had an M2-like (anti-inflammatory) phenotype than animals treated with control-np, with M2-like macrophages representing 18% of macrophages from animals treated with Control-np, but 33% of macrophages from animals treated with NO-np (b). (a) n = 650 macrophages/group, (b) n = 585 macrophages/group.

over 72% of macrophages tested via FACS presented an M1-like phenotype for animals treated with control-np, but only 16% of macrophages represented an M1-like phenotype for animals treated with NO-np. However, animals treated with NO-np showed a larger population of M2-like macrophages (representing 33% of macrophages harvested), which are typically considered to be anti-inflammatory, and are associated with tissue repair. To supplement these macrophage phenotypes, we also measured the cytokine profile of treated mice after LPS injection.

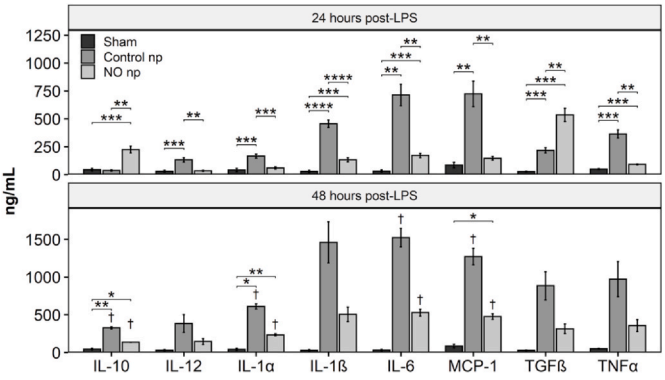

Fig. 6. Cytokine profile of mice treated with NO-np and Control-np after LPS dosage after 24 and 48 h. At 24 h, anti-inflammatory cytokines (IL-10, TGFβ) were significantly higher in animals treated with NO-np compared to Control-np, but inflammatory cytokines showed an opposite trend. Data are presented as mean ± SD. Data between groups and between time points were analyzed with Welch's t-tests with Bonferroni correction. N = 4/group at 24 h & N = 2/group at 48 h for animals dosed with LPS; N = 3 for Sham at both time points. *p < 0.05, **p < 0.01, ***p < 0.001, and ****p < 0.0001 between groups; †p < 0.05 vs 24 h post-LPS.

3.7. Cytokine profile

Cytokines were measured 24 and 48 h after LPS injection (Fig. 6). After 24 h, animals treated with NO-np showed significantly higher levels of cytokines traditionally considered to be anti-inflammatory (interleukin [IL]-10, TGF-beta), and significantly lower levels of cytokines associated with a proinflammatory response (IL-1, 6, 12, MCP, and TNF alpha) than animals treated with Control-np. However, after 48 h, all cytokines measured were elevated in animals dosed with Control-np compared to NO-np, but not all of these comparisons were statistically significant.

4. Discussion

The principle finding of this study is that sustained delivery of exogenous NO using NO releasing nanoparticles improved microvascular flow and capillary transit compared to animals treated with control nanoparticles during LPS-induced endotoxemia. Additionally, this study demonstrates that the adverse microcirculatory changes from LPS-induced endotoxemia precede systemic changes by hours. NO-np also significantly improved 72-h survival of mice after LPS-induced endotoxemia. Additionally, treatment with NO-np caused macrophages to shift toward an anti-inflammatory (M2-like) phenotype, while macrophages of animals treated with Control-np were consistent with an inflammatory (M1-like) phenotype. In general, treatment with NO-np significantly ameliorated the effects of LPS-induced endotoxemia, and could be a treatment for sepsis or other systemic inflammatory conditions.

Systemic changes seen in this study were consistent with other studies of sepsis and LPS-induced endotoxemia, and included severe hypotension and bradycardia for both experimental groups [4,9,15]. Additionally, we observed arteriolar dilation in the microcirculation, and a reduction in the volumetric flow rate, independent of treatment. The decrease in FCD, and thus tissue perfusion, seen in this experiment preceded any systemic changes. As such, a decrease in FCD is likely the trigger that allows sepsis to progress to the clinical manifestations of severe sepsis and septic shock. Preserving FCD is therefore key to improving outcomes from systemic inflammatory diseases, like sepsis. NO-np treatment partially ameliorated this decrease in FCD, and as such could be a plausible treatment for acute systemic inflammatory

conditions, such as sepsis, hemorrhagic shock, and COVID-19 infection.

There are a number of mechanisms that may be responsible for the improved survival and maintenance of microvascular perfusion seen with NO-np treatment in this study, but the exact mechanism or set of mechanisms is unclear. As we saw, and as others have demonstrated [22], NO treatment decreased M1, and increased M2 polarization of macrophages. This can have a multitude of downstream effects as M1 macrophages produce proinflammatory cytokines, upregulate inducible nitric oxide synthase (iNOS), and enhance production of ROS and reactive nitrogen species, which disrupt the glycocalyx, expose the endothelial layer, decrease NO production from eNOS, and destroy endothelial cells [23,24].

Disruption of the glycocalyx undermines vascular integrity and eliminates the shear stress-based trigger for production of NO from eNOS. Mice treated with Control-np in our study experienced significantly increased vascular permeability, as shown in Fig. 4, suggesting endothelial cell and glycocalyx disruption in these animals. The glycocalyx has a number of vital physiological roles, including acting as a barrier to preserve intravascular oncotic pressure [23], promoting RBC marginalization and the presence of a red cell-free layer [25,26], reducing leukocyte adhesion and infiltration [26], and preventing thrombus formation and attachment [27], so its disruption is likely a primary determinant for many of the clinical presentations of sepsis, such as edema. As such, it is logical that the glycocalyx has been a common drug target in improving outcomes from sepsis. Others have explored individual mechanisms as a method to prevent glycocalyx degradation during sepsis, but these strategies have not shown much clinical success [23]. However, NO-np treatment seems particularly promising as it attempts to treat a more upstream target than previous therapies by preventing the initial insult to the glycocalyx, and thus preserving endogenous NO signaling. Endogenous NO may function to upregulate and activate nuclear factor erythroid 2-related factor 2 (Nfr2) which represents a potent signaling pathway to counter an LPS-induced inflammatory cascade, and to down regulate pro-inflammatory pathways and thus decrease ROS production [28]. The observed NO-induced macrophage repolarization is indicative of the potential role endogenous NO may play in decreasing ROS and cytokine production by activated macrophages.

NO-np treatment also likely improves outcomes from sepsis by reducing the hypercoagulable state. Sepsis also induces a hypercoagulable state, with thrombi potentially forming in the microcirculation of the lungs, heart, and kidneys of sepsis patients [29]. These thrombi are mediated and formed as a result of tissue injury, which promotes clotting via the extrinsic pathway, direct activation of platelets from inflammatory cytokines, damage to RBCs from reactive oxygen species released by leukocytes, and from the aforementioned degradation of the endothelial glycocalyx, culminating in thrombi formation and adhesion to the exposed endothelial layer of vessels [29,30]. However, NO likely played a protective role against coagulopathies in this study. NO is known to block platelet activation, alter clot formation time and strength, and protect against reocclusion after thrombolysis [31–34]. This, in combination with M2 polarization of macrophages and the possible prevention of glycocalyx degradation by exogenous NO supplementation, all may have contributed to a potential decrease in coagulopathy, and thus improved microvascular flow for animals treated with NO-np.

It is likely that NO-np treatment contributed to these two mechanisms – the preservation of the glycocalyx and prevention of coagulopathies – which improved FCD and thus tissue perfusion observed in this study. Preserving the endothelial glycocalyx during sepsis improves microvascular blood flow by preventing leukocyte adhesion, promoting RBC marginalization, and improving fluid homeostasis. Additionally, preventing coagulopathies preserves FCD, as capillaries can only transport a single cell at a time, and thrombi can easily block capillaries. This study showed that the preservation of FCD via treatment with NO-np improved survival compared to animals treated with Control-np. Others have shown that microvascular perfusion is central in preventing multi-organ dysfunction syndrome (MODS), which is a key player in sepsis progression [35]. It is also possible that NO-np treatment mildly improved cardiac function: despite significantly increased perfusion (as indicated by FCD) and thus decreased vascular resistance, MAP was the same for both groups; as such, cardiac output must be increased in the NO-np group compared to the Control-np group.

Other groups have also shown success in treating systemic inflammatory conditions, including sepsis, with NO and NO donors. For example, Spronk et al. showed that nitroglycerin, an NO donor, improved microvascular flow when given with fluid resuscitation [36], and others showed that nitrite also protects against septic shock [37]. A multitude of other therapies for sepsis have been explored, including ATP, activated protein C, and simvastatin with promising results [6]. Ultimately, NO releasing nanoparticles seem to be a promising treatment for sepsis, as they are safer and easier to handle and administer than alternatives, can be prepared in a cost-effective manner, and they target upstream mechanisms, rather than the downstream consequences.

The results of this study have implications for other acute systemic inflammatory conditions such as hemorrhagic shock due to the proinflammatory triggers associated with both ischemia-reperfusion and hypoxia-reoxgenation injuries. Indeed we have recently shown that exogenously delivered NO targeted to the site of an induced ischemic insult prevented the usual inflammatory consequences [38]. The observed array of clinical manifestations associated with Corona Virus Disease 2019 (COVID-19) that correspond to many of the anticipated consequences of systemic endothelial dysfunction due to a cytokine storm is relevant when discussing exogenous NO treatments during LPS-induced endotoxemia [39]. We see in the present study that NO can function to repolarize activated macrophages and reduce inflammation. Based on the present study, it would appear that the absence of NO production due to ACE2 deactivation during COVID-19 can account for the hypercoagulopathies, tissue hypoxia, and extreme vascular leakage observed in COVID-19. A plausible mechanism for the clinical consequences of COVID-19 is the combination of the strong proinflammatory trigger initiated by viral overload and the deactivation of ACE2 by the virus [40]. The virus that causes COVID-19 uses ACE2, the initiator of the inflammatory shutdown process, as a binding site for entry into cells [41,42]. A consequence of the viral binding to ACE2 is the deactivation of ACE2, thus eliminating the braking mechanism for virus-induced inflammation [43]. A key element of the ACE2 anti-inflammatory signaling mechanism is the upregulation of eNOS with a concomitant increase in NO production [44]. As such, the present study implies that exogenous NO or agents that stimulate NO formation in the endothelium may play a role in limiting the extreme manifestations of COVID-19 likely in part through activation of Nrf 2. In fact, the US Food and Drug Administration has recently approved NO and NO donor therapy for expanded emergency access for the treatment of COVID-19 [45].

Limitations. LPS induced endotoxemia does not fully replicate the cascade of events that occurs during septic shock, but no study can fully replicate the morbidity of septic shock due to its distinct etiologies. However, this study did demonstrate that this mouse model replicates many of the early changes that occur in septic shock, including increased vascular permeability, and impaired systemic oxygen transport, and allowed us to observe these changes in an awake, unanesthetized model. Since anesthetics have a poorly characterized influence on inflammation, the awake unanesthetized state is most representative of changes that may occur during sepsis. Unfortunately, this study did not measure any parameters examining the status of the vascular endothelial glycocalyx, since sepsis damages the glycocalyx, and exogenous NO could help protect the glycocalyx. Future studies should examine changes in the glycocalyx by measuring its breakdown molecules, such as heparan sulfate and sydecan-1, in the plasma, or measure

glycocalyx integrity and thickness via fluorescent lectin binding, in order to directly study glycocalyx disruption during LPS-induced endotoxemia, and its protection by NO-nps.

5. Conclusion

This study demonstrated that NO-np improved outcomes from LPS-induced endotoxemia. Additionally, this study showed the importance of measuring microvascular outcomes in systemic inflammatory conditions, as we saw adverse microcirculatory events occur hours before systemic changes, and systemic hemodynamics were not predictive of 72-h survival. Overall, the results indicate that exogenous NO has potential as a therapeutic modality to limit the inflammatory progression for many acute pro-inflammatory triggers.

Author contributions

ATW, JMF, and PC wrote the main manuscript text. ATW, CRM, and KG analyzed the data. ATW prepared the figures. JMF, AJF, and PC contributed to the design and implementation of the experiment. AJF and MSN prepared and characterized nanoparticles. All authors reviewed and revised the manuscript. All authors approved of the manuscript text.

Funding

This work was supported by the NIH Heart Lung and Blood Institute under grants R01-HL126945, and R01-HL138116.

Declaration of competing interest

AJF, MSN, and JMF hold patents related to the production and use of nitric-oxide releasing nanoparticles. All other authors declare no conflicts of interest related to the work presented in this manuscript.

Acknowledgements

The authors would like to thank Cynthia Walser (UC San Diego) for surgical preparation of the animals.

References

[1] J.E. Parrillo, Pathogenetic mechanisms of septic shock, N. Engl. J. Med. 328 (1993) 1471–1477.
[2] D.C. Angus, W.T. Linde-Zwirble, J. Lidicker, G. Clermont, J. Carcillo, M.R. Pinsky, Epidemiology of severe sepsis in the United States: analysis of incidence, outcome, and associated costs of care, Crit. Care Med. 29 (2001) 1303–1310.
[3] F.B. Mayr, S. Yende, D.C. Angus, Epidemiology of severe sepsis, Virulence 5 (2014) 4–11.
[4] D.C. Angus, T. van der Poll, Severe sepsis and septic shock, N. Engl. J. Med. 369 (2013) 840–851.
[5] W.L. Lee, A.S. Slutsky, Sepsis and endothelial permeability, N. Engl. J. Med. 363 (2010) 689–691.
[6] J.R. Jacobson, J.G.N. Garcia, Novel therapies for microvascular permeability in sepsis, Curr. Drug Targets 8 (2007) 509–514.
[7] C. Ince, The microcirculation is the motor of sepsis, Crit. Care 9 (2005) S13.
[8] G. Hernandez, E.C. Boerma, A. Dubin, A. Bruhn, M. Koopmans, V.K. Edul, C. Ruiz, R. Castro, M.O. Pozo, C. Pedreros, E. Veas, A. Fuentealba, E. Kattan, M. Rovegno, C. Ince, Severe abnormalities in microvascular perfused vessel density are associated to organ dysfunctions and mortality and can be predicted by hyperlactatemia and norepinephrine requirements in septic shock patients, J. Crit. Care 28 (2013) 538 e9–14.
[9] R.M. Bateman, K.R. Walley, Microvascular resuscitation as a therapeutic goal in severe sepsis, Crit. Care 9 (2005) S27.
[10] P. Cabrales, P. Nacharaju, B.N. Manjula, A.G. Tsai, S. a Acharya, M. Intaglietta, Early difference in tissue pH and microvascular hemodynamics in hemorrhagic shock resuscitation using polyethylene glycol-albumin- and hydroxyethyl starch-based plasma expanders, Shock 24 (2005) 66–73.
[11] B. Fagrell, M. Intaglietta, Microcirculation: its significance in clinical and molecular medicine, J. Intern. Med. 241 (5) (1997) 349–362.
[12] G. Guven, M.P. Hilty, C. Ince, Microcirculation: physiology, pathophysiology, and clinical application, Blood Purif. 49 (2020) 143–150.
[13] R. Bezemer, S.A. Bartels, J. Bakker, C. Ince, Clinical review: clinical imaging of the sublingual microcirculation in the critically ill - where do we stand? Crit. Care 16 (2012) 224.
[14] Y.-C. Lu, W.-C. Yeh, P.S. Ohashi, LPS/TLR4 signal transduction pathway, Cytokine 42 (2008) 145–151.
[15] J.A. Buras, B. Holzmann, M. Sitkovsky, Animal Models of sepsis: setting the stage, Nat. Rev. Drug Discov. 4 (2005) 854–865.
[16] A.J. Friedman, G. Han, M.S. Navati, M. Chacko, L. Gunther, A. Alfieri, J.M. Friedman, Sustained release nitric oxide releasing nanoparticles: characterization of a novel delivery platform based on nitrite containing hydrogel/glass composites, Nitric Oxide 19 (2008) 12–20.
[17] P. Nacharaju, C. Tuckman-Vernon, K.E. Maier, J. Chouake, A. Friedman, P. Cabrales, J.M. Friedman, A nanoparticle delivery vehicle for S-nitroso-N-acetyl cysteine: sustained vascular response, Nitric Oxide 27 (2012) 150–160.
[18] P. Cabrales, G. Han, C. Roche, P. Nacharaju, A.J. Friedman, J.M. Friedman, Sustained release nitric oxide from long-lived circulating nanoparticles, Free Radic. Biol. Med. 49 (2010) 530–538.
[19] B. Endrich, K. Asaishi, A. Götz, K. Meßmer, Technical report—a new chamber technique for microvascular studies in unanesthetized hamsters, Res. Exp. Med. 177 (1980) 125–134.
[20] A. Sckell, M. Leunig, Dorsal skinfold chamber preparation in mice: studying angiogenesis by intravital microscopy, Methods Mol. Biol. 1430 (2016) 251–263.
[21] D. Ortiz, J.C. Briceno, P. Cabrales, Microhemodynamic parameters quantification from intravital microscopy videos, Physiol. Meas. 35 (2014) 351–367.
[22] W.J. Lee, S. Tateya, A.M. Cheng, N. Rizzo-DeLeon, N.F. Wang, P. Handa, C.L. Wilson, A.W. Clowes, I.R. Sweet, K. Bomsztyk, M.W. Schwartz, F. Kim, M2 macrophage polarization mediates anti-inflammatory effects of endothelial nitric oxide signaling, Diabetes 64 (2015) 2836–2846.
[23] C. Chelazzi, G. Villa, P. Mancinelli, A.R. De Gaudio, C. Adembri, Glycocalyx and sepsis-induced alterations in vascular permeability, Crit. Care 19 (2015) 26.
[24] F.O. Martinez, S. Gordon, The M1 and M2 paradigm of macrophage activation: time for reassessment, F1000Prime Rep 6 (2014).
[25] O. Yalcin, V.P. Jani, P.C. Johnson, P. Cabrales, Implications enzymatic degradation of the endothelial glycocalyx on the microvascular hemodynamics and the arteriolar red cell free layer of the rat cremaster muscle, Front. Physiol. 9 (2018).
[26] A. Constantinescu Alina, Hans Vink, A.E. spaan Jos, Endothelial cell glycocalyx modulates Immobilization of leukocytes at the endothelial surface, Arterioscler. Thromb. Vasc. Biol. 23 (2003) 1541–1547.
[27] R. Uchimido, E.P. Schmidt, N.I. Shapiro, The glycocalyx: a novel diagnostic and therapeutic target in sepsis, Crit. Care 23 (2019) 16.
[28] G.E. Mann, D.J. Rowlands, F.Y.L. Li, P. de Winter, R.C.M. Siow, Activation of endothelial nitric oxide synthase by dietary isoflavones: role of NO in Nrf 2-mediated antioxidant gene expression, Cardiovasc. Res. 75 (2007) 261–274.
[29] J. Simmons, J.-F. Pittet, The coagulopathy of acute sepsis, Curr. Opin. Anaesthesiol. 28 (2015) 227–236.
[30] B. Dixon, The role of microvascular thrombosis in sepsis, Anaesth. Intensive Care 32 (2004) 619–629.
[31] S.K. Yao, S. Akhtar, T. Scott-Burden, J.C. Ober, P. Golino, L.M. Buja, W. Casscells, J.T. Willerson, Endogenous and exogenous nitric oxide protect against intracoronary thrombosis and reocclusion after thrombolysis, Circulation 92 (1995) 1005–1010.
[32] K. Matsushita, C.N. Morrell, B. Cambien, S.-X. Yang, M. Yamakuchi, C. Bao, M.R. Hara, R.A. Quick, W. Cao, B. O'Rourke, J.M. Lowenstein, J. Pevsner, D.D. Wagner, C.J. Lowenstein, Nitric oxide regulates exocytosis by S-Nitrosylation of N-ethylmaleimide-Sensitive factor, Cell 115 (2003) 139–150.
[33] J.E. Freedman, J. Loscalzo, Nitric oxide and its relationship to thrombotic disorders, J. Thromb. Haemostasis 1 (2003) 1183–1188.
[34] C.C. Helms, S. Kapadia, A.C. Gilmore, Z. Lu, S. Basu, D.B. Kim-Shapiro, Exposure of fibrinogen and thrombin to nitric oxide donor ProliNONOate affects fibrin clot properties, Blood Coagul. Fibrinolysis 28 (2017) 356–364.
[35] C.J. Kirkpatrick, F. Bittinger, C.L. Klein, S. Hauptmann, B. Klosterhalfen, The role of the microcirculation in multiple organ dysfunction syndrome (MODS): a review and perspective, Virchows Arch. 427 (1996) 461–476.
[36] P.E. Spronk, C. Ince, M.J. Gardien, K.R. Mathura, H.M.O. Straaten, D.F. Zandstra, Nitroglycerin in septic shock after intravascular volume resuscitation, Lancet 360 (2002) 1395–1396.
[37] A. Cauwels, E.S. Buys, R. Thoonen, L. Geary, J. Delanghe, S. Shiva, P. Brouckaert, Nitrite protects against morbidity and mortality associated with TNF- or LPS-induced shock in a soluble guanylate cyclase–dependent manner, J. Exp. Med. 206 (2009) 2915–2924.
[38] M.S. Navati, A. Lucas, C. Liong, M. Barros, J.T. Jayadeva, J.M. Friedman, P. Cabrales, Reducing ischemia/reperfusion injury by the targeted delivery of nitric oxide from magnetic-Field-induced Localization of S-Nitrosothiol-Coated paramagnetic nanoparticles, ACS Appl. Bio Mater. 2 (2019) 2907–2919.
[39] P. Mehta, D.F. McAuley, M. Brown, E. Sanchez, R.S. Tattersall, J.J. Manson, COVID-19: consider cytokine storm syndromes and immunosuppression, Lancet 395 (2020) 1033–1034.
[40] H. Kai, M. Kai, Interactions of coronaviruses with ACE2, angiotensin II, and RAS inhibitors—lessons from available evidence and insights into COVID-19, Hypertens. Res. (2020) 1–7.
[41] M. Hoffmann, H. Kleine-Weber, S. Schroeder, N. Krüger, T. Herrler, S. Erichsen, T.S. Schiergens, G. Herrler, N.-H. Wu, A. Nitsche, M.A. Müller, C. Drosten, S. Pöhlmann, SARS-CoV-2 cell entry depends on ACE2 and TMPRSS2 and is blocked by a clinically proven protease Inhibitor, Cell 181 (2020) 271–280 e8.
[42] A.C. Walls, Y.-J. Park, M.A. Tortorici, A. Wall, A.T. McGuire, D. Veesler, Structure, function, and antigenicity of the SARS-CoV-2 spike glycoprotein, Cell 181 (2020)

281–292 e6.
[43] K. Kuba, Y. Imai, S. Rao, H. Gao, F. Guo, B. Guan, Y. Huan, P. Yang, Y. Zhang, W. Deng, L. Bao, B. Zhang, G. Liu, Z. Wang, M. Chappell, Y. Liu, D. Zheng, A. Leibbrandt, T. Wada, A.S. Slutsky, D. Liu, C. Qin, C. Jiang, J.M. Penninger, A crucial role of angiotensin converting enzyme 2 (ACE2) in SARS coronavirus-induced lung injury, Nat. Med. 11 (2005) 875–879.
[44] L.A. Rabelo, N. Alenina, M. Bader, ACE2-angiotensin-(1-7)-Mas axis and oxidative stress in cardiovascular disease, Hypertens. Res. 34 (2011) 154–160.
[45] N.C. Adusumilli, D. Zhang, J.M. Friedman, A.J. Friedman, Harnessing nitric oxide for preventing, limiting and treating the severe pulmonary consequences of COVID-19, Nitric Oxide 103 (2020) 4–8.